

A mesoscopic device for a realization of the Topological Kondo effect

Saheli Sarkar¹ and Alexei M. Tsvelik¹

¹*Division of Condensed Matter Physics and Materials Science,
Brookhaven National Laboratory, Upton, NY 11973-5000, USA*

The search for anyons is a field of immense interest owing to its potential application in the field of quantum information. Quantum critical Kondo impurities constitute one possible platform for their realization and Topological Kondo effect (TKE) by virtue of remaining critical in the presence of perturbations, seems to be especially promising in this regard. In this paper we discuss practical steps for a realization of TKE with a relatively high Kondo temperature T_K . Its central feature is the so-called Majorana-Cooper box (MCB) and we argue that a particular type of iron-based topological superconductor is especially suitable for realization of TKE. Once MCB is available one needs to connect it to external metallic leads to produce TKE. A relatively high value of the Kondo temperature T_K is then aided by a large superconducting gap of the iron-based superconductor. We give estimates for T_K , for the cases of both isotropic and anisotropic exchange couplings of MCB with the leads.

I. INTRODUCTION

Anyons - fractionalized particles with exotic statistics, are considered an essential part of quantum information systems [1]. There are different suggestions of their realization, one of them being the Kondo effect. Existence of quantum critical Kondo effect with a non-Fermi liquid (NFL) behavior, first described and studied theoretically [2–4] has been well established experimentally [5–9]. It is well understood that the corresponding critical ground state contains non-Abelian anyons [10–12]. However, the experiments implement the so-called multichannel Kondo effect where the criticality is sensitive to asymmetry between the scattering channels. Hence a realization of the quantum critical point requires a fine tuning of the coupling parameters which limits its potential applications.

Béri and Cooper *et.al.* [13] proposed a new type of non-Fermi liquid Kondo effect where the criticality is stable against most common perturbations. The Topological Kondo effect (TKE) is predicted to arise as a result of coupling between bulk conduction electrons and Majorana Zero modes [MZM, also called Majorana Bound States (MBSs)] located inside of the so-called Majorana-Cooper box (MCB). They also provided a sketch of the MCB setup for TKE [13] in the form of a device consisting of a mesoscopic superconducting island with proximitized to it semiconductor nanowires containing the MBSs. The Coulomb blockade in the island transforms entangled MBSs into an effective quantum spin, which interacts with the conduction electrons of the leads via superexchange interaction facilitating the TKE. In contrast to the conventional quantum critical Kondo effect, the TKE is robust against various perturbations [14, 15].

Apart from being an anyon platform, the TKE with its characteristic features may resolve persistent controversies about the existence of MBS. The theory [13, 14] suggests that in the device with M leads, the linear conductance (σ_{ij}) between different leads i and j saturates at small temperatures at the universal value $\frac{2e^2}{Mh}$, following a nontrivial power law temperature dependence, different from the T^2 Fermi liquid one. This universal behavior of the conductance constitutes a manifestation of the anyonic character of the TKE ground state, which therefore can serve as a smoking gun for the presence

of MBS.

The aim of this paper is to provide detailed suggestions for realization of MCBs for TKE focusing on iron-based superconductors (FeSC) based systems, with a final goal to use it for quantum information applications. We provide different scenarios for realizing MCBs using FeSC and parameters characterizing the device for realizing TKE, in the absence and presence of anisotropy of the exchange couplings between MCB and the external metallic leads. We also depict an arrangement for a TKE-based chiral Kondo lattice which contains multiple non-Abelian anyons.

As we have mentioned above, the suggestions of realization of TKE contained in earlier theoretical studies described heterostructure devices containing nanowires with strong spin-orbit interaction in the presence of magnetic field proximitized to a mesoscopic size superconducting island [13, 15–17]. We suggest another route to TKE: to use intrinsic topological superconductor (TSC) [18–20] based devices, which may naturally host Majorana fermions. This may drastically simplify the fabrication process providing a material realization for the TKE. Promising candidates include iron-based superconductors $\text{Fe}(\text{Te}_x, \text{Se}_{1-x})$ ($T_c = 14.5$ K) [21–23], $(\text{Li}_{0.84}\text{Fe}_{0.16})\text{OHFeSe}$ ($T_c = 42$ K) [24] and $\text{CaKFe}_2\text{As}_4$ ($T_c = 35$ K) [25]. All of them exhibit signatures of intrinsic topological superconductivity and have relatively high superconducting critical temperatures T_c . Thus, it is conceivable that MCB based on such materials can provide a viable path towards observing the TKE. Observation of TKE in turn can serve as a smoking gun signature of MBS, whose detection in various systems has been so far largely focused on observing a zero-bias conductance peak (ZBCP)[26, 27] in local probe techniques. Additionally, finding signatures of non-local character [28] of MBS through TKE will be important for quantum computation applications.

II. DIFFERENT SCENARIO FOR REALIZATION OF MAJORANA-COOPER BOXES

There are multiple experiments indicating a possible existence of MBSs in various iron-based superconductors. Non of them are decisive, but as we suggest, in the context of

TKE the corresponding systems may provide smoking gun evidence for MBS. Below we consider different arrangements weighting their merits as possible candidates for realization of TKE. In all cases the corresponding MCBs are conceived as mesoscopic devices consisting of superconductor with charging energy E_C containing MBSs.

Vortices: One way of coexistence of MBSs and superconductivity is through vortices. There are multiple observations of ZBCP trapped in vortex cores of superconductors $\text{Fe}(\text{Te}_x, \text{Se}_{1-x})$ [21–23], $(\text{Li}_{0.84}\text{Fe}_{0.16})\text{OHFeSe}$ [24] and $\text{CaKFe}_2\text{As}_4$ [25]. These experiments are interpreted as evidence for MBS. However, there are several difficulties in clearly distinguishing the MBSs, for e.g. due to the presence of topologically trivial Caroli-de Gennes- Matricon [29] states at the vortex cores. The Caroli-de Gennes- Matricon states are observed to produce a broad peak centering at the zero energy, as the energy separation between the states is of the order of Δ^2/E_F , where E_F is the Fermi energy. Thus as the energy separation can be significantly smaller than the instrumental energy resolution, they appear as a broad peak at the zero energy, being different in origin from that of the MBS. Moreover, scanning-tunneling microscopy (STM) experiments [23, 30] in $\text{FeSe}_{0.45}\text{Te}_{0.55}$ have reported the presence of the ZBCP only in a fraction of the vortex cores present in the system, depending on the magnetic field, rendering the MBSs questionable.

Magnetic point defects: Quantum anomalous vortices [31] may nucleate at magnetic impurities at zero magnetic field. In the presence of a surface topological superconductivity they can support MBSs at the vortex centers, manifesting themselves as ZBCP in tunneling experiments. These types of sharp zero energy peaks located at interstitial iron impurities (IFI) have been observed by STM in the superconducting state of $\text{Fe}_{1+x}(\text{Te}, \text{Se})$ [26] with superconducting gap of about 2 meV, below superconducting temperature $T_c = 14.5$ K. The zero bias peak intensity decays exponentially from the center of the peak with correlation length $\xi \approx 3.5$ Å, which is much smaller than the superconducting correlation length ~ 25 Å. The STM have found IFIs on the exposed (Te, Se) surface located right at the mid position between four neighboring (Te, Se) atoms. They manifest themselves as sharp peaks at zero bias; the peaks remain robust in applied magnetic field up to 8 T. Similar ZBCP have also been found later in LiFeAs [32] and in IFI on monolayers of FeSe and $\text{FeSe}_{0.5}\text{Te}_{0.5}$ on SrTiO_3 (STO) [33]. One potential problem is that the peak has an intrinsic width in all of the systems [for e.g., in $\text{Fe}_{1+x}(\text{Te}, \text{Se})$ [26] the width ~ 0.6 meV at $T = 1.5$ K] whose origin is unclear. Perhaps, this widening can be taken into account phenomenologically as a result of a coupling of the MBS to the bath. In any case, it will likely to have a damaging effect on TKE. Additionally, in a STM experiment [34] in $\text{FeSe}_{0.45}\text{Te}_{0.55}$ with IFI, the ZBCP was found only near some iron adatoms, the rest of them having Yu-Shiva- Rusinov (YSR) bound states at finite energies.

Line defects: The STM study [35] reports a discovery of zero-energy bound states simultaneously appearing at both ends of a one-dimensional atomic line defect in monolayer iron-based high-temperature superconductor

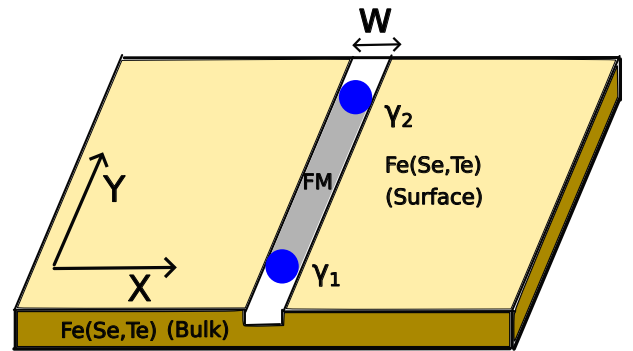


FIG. 1: A schematic representation of a mesoscopic setup for the formation of a paired Majorana bound states: The device contains a slab of $\text{Fe}(\text{Se}, \text{Te})$ superconductor and a ferromagnetic film (FM) of width W deposited on the surface of the superconductor, with W being much smaller than the size of the superconductor. This effectively gives rise to a superconductor-ferromagnet-superconductor (S-F-S) junction.

$\text{FeTe}_{0.5}\text{Se}_{0.5}$ films grown on $\text{SrTiO}_3(001)$ substrates, which has $T_c \approx 62$ K. These line defects naturally emerge during the growth process and correspond to lines of missing Te/Se atoms.

Another recent STM [36] study has found evidence of Majorana fermions in a certain type of crystalline domain walls associated to the half-unit cell shift of the Se atom in superconducting $\text{FeSe}_{0.45}\text{Te}_{0.55}$ [$\text{Fe}(\text{Se}, \text{Te})$]. It was established in [37], this material also develops surface ferromagnetism. The first principle calculations [38] have suggested that these types of crystalline domain walls can develop an in-plane ferromagnetism along the domain wall orientation and may support Majorana modes. Moreover, it has been also suggested, that if the magnetization can be tuned, MBS can be trapped by defects such as ferromagnetic domain wall [38].

Motivated by these, we consider a model device consisting of a mesoscopic $\text{Fe}(\text{Se}, \text{Te})$ and a ferromagnetic film, which can be used to study TKE with a higher Topological Kondo temperature scale, thus providing advantage of previously proposed setup based on complex heterostructures.

Below we describe in detail the setup of a device giving rise to a pair of MBS's. It is composed of a slab of $\text{Fe}(\text{Se}, \text{Te})$ material and a thin ferromagnetic film (FM) deposited on the surface of the $\text{Fe}(\text{Se}, \text{Te})$ or any similar material as shown in the Fig.1. Below the T_c , one part of the device becomes superconducting, in the thin film area, however, the ferromagnetism persists. Hence, the system can be simply modeled as a superconductor-ferromagnet-superconductor (S-F-S) junction [see Fig.1]. In the Fig. 1, the x-axis points to the normal to the junction between the ferromagnet and the superconductor, whereas the y-axis points parallel to the orientation of the junction. The semi-infinite superconducting regions occupy intervals $x < -W/2$ and $x > W/2$, while the FM region occupies interval $-W/2 < x < W/2$. We consider that the system size along y-direction as infinite, the width W remains finite. The $\text{Fe}(\text{Se}, \text{Te})$ is known to have non-trivial topologi-

cal spin-helical Dirac surface states [22] as well as the Rashba type spin-orbit coupling [39, 40]. The bulk of Fe(Se,Te) possesses a node-less and almost isotropic s-wave type superconducting gap [41]. The FM produces an effective Zeeman field h_y parallel to the junction.

Consequently, the surface S-F-S junction of width W is described by the following Dirac-Bogolyubov-de-Gennes (BdG) Hamiltonian [38] in the Nambu basis $\Psi = (\psi_{k,\uparrow}^\dagger, \psi_{k,\downarrow}^\dagger, \psi_{-k,\uparrow}, \psi_{-k,\downarrow})$:

$$H_{BdG} = \begin{pmatrix} H_0(k) & i\sigma_y \Delta(r) \\ -i\sigma_y \Delta^*(r) & -H_0^*(-k) \end{pmatrix} \quad (1)$$

In Eqn.(1), $H_0(k)$ is a 2×2 matrix, $H_0(k) = H_{SO} - \mu + H_Z(x)$. The $H_0(k)$ contains the Rashba spin-orbit coupling term $H_{SO} = \alpha(\sigma \times k) \cdot \hat{z}$, associated to the Dirac surface states of the Fe(Se,Te), a chemical potential μ and a Zeeman energy term due to the FM given by $H_Z(x) = \sigma_y h_y \Theta[(W/2) - |x|]$. Here, $\alpha = v_F \hbar$, is the coupling strength, and v_F is the Fermi velocity. σ are the Pauli matrices in the spin-space. With $\hbar = 1$, the Rashba term H_{SO} becomes $v_F(\sigma_x k_y + i\sigma_y \partial_x)$, where k_y is momentum along the y-direction that is conserved in the system. The spatial variation of the superconducting gap function on the surface satisfies $\Delta(r) = \Delta_0 e^{i\text{sgn}(x)(\theta/2)} \Theta[|x| - W/2]$, where θ is the phase difference between the left and the right superconducting regime.

It has been shown in [38], that the S-F-S junction described by the Hamiltonian Eqn.(1) can support one dimensional counter propagating Majorana modes for a constant phase difference ($\Delta\phi = \pi$) between the two superconducting regimes on the left and right arising due to the in-plane magnetic moment in the FM. Moreover, the localized MBSs are formed [42] from the coupling between these dispersive Majorana modes, if the phase difference $\Delta\phi(y)$ varies continuously along the orientation y of the junction such that, $\Delta\phi(y)$ becomes an odd integer multiple of π . This follows from the analysis of the low energy effective Hamiltonian derived from the BdG Hamiltonian Eqn.(1), by projecting it onto the basis of the one-dimensional Majorana modes [38]:

$$H_{eff} = v_m k_y \tau_y - \Delta_0 \cos \left[\frac{\Delta\phi(y)}{2} \right] \tau_z, \quad (2)$$

$$\Delta\phi(y) = \frac{2h_y W}{v_F}, \quad (3)$$

$$v_m = v_F \left[\cos k_F W + \frac{\Delta_0}{\mu} \sin k_F W \right] \frac{\Delta_0^2}{(\mu^2 + \Delta_0^2)} \quad (4)$$

, where τ are the Pauli matrices in the particle-hole space. Note that the Eqn.(2) has the form of a Su-Schrieffer-Heeger model. It is also well-known from the Jackiw-Rabbi problem, that a zero energy localized MBS forms when the mass term $\Delta_0 \cos(\frac{\Delta\phi(y)}{2})$ in Eqn.(3) smoothly changes sign or $\Delta\phi(y)$ becomes an odd integer multiple of π . The Bogoliubov quasiparticle operator associated with this state is a Majorana fermion, which satisfies $\gamma_0 = \gamma_0^\dagger$.

Therefore in this setup, to tune the phase difference $\Delta\phi(y)$

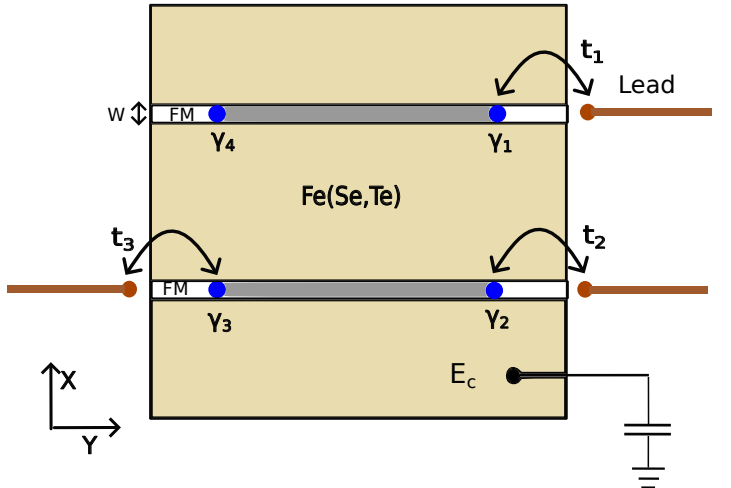


FIG. 2: A schematic representation of a mesoscopic setup for Topological Kondo effect with $N = 4$ MBSs and $M = 3$ metallic leads: The device contains a Coulomb blockaded superconducting island made of Fe(Se,Te) superconductor and FM. The island is connected to the ground through a capacitor and hence possesses a charging energy E_c . 3 MBSs are tunnel coupled to the metallic leads with coupling constants t_j 's ($j = 1, 2, 3$).

for obtaining a pair of MBSs, either the width W of the FM can be changed along the y direction or a soft magnetic material for the FM can be used where one can vary the magnetization strength h_y .

III. A FeSC -BASED DEVICE FOR OBSERVATION OF TOPOLOGICAL KONDO EFFECT

The MCB device considered in our work for the realization of the Topological Kondo effect (TKE) comprises of a mesoscopic Fe(Se,Te) (or a similar material) and two ferromagnetic films deposited on it and resulting in a pair of MBS in each of the ferromagnetic films as shown in Fig. 2. Realization of the TKE suggested in the Ref.[13] is based on the MCB which was described, for example, in [43], containing $N \geq 4$ MZMs. Following the suggestions, we consider a floating mesoscopic MCB island, grounded through a capacitor. To get the critical ground state, one needs to connect MZMs to just three external metallic leads (this is a minimal number) via tunneling contacts as schematically depicted in Fig. 2. The charging energy $E_C = \frac{e^2}{2C}$, with C being the geometric capacitance of the box, contributes to the Hamiltonian of the MCB island as

$$H_c = E_c(N - Q_0/e)^2. \quad (5)$$

In Eqn.(5), N is the number of electrons in the island and Q_0 is the background charge determined by the voltage across the capacitor, connected to the MCB.

In general, if there are a total N number of MBS in the

MCB, there will be $N/2$ number of zero energy fermionic modes. As the total charge of the island is fixed by a large charging energy E_c , to even or odd number, thus gives a parity constraint to the MBS operators. This leads to a ground state of the system with $2^{(N/2)-1}$ fold degeneracy. In this work, we consider the arrangement where MCB island contains four Majorana zero modes $N = 4$, hence the ground state is two-fold degenerate. The two degenerate quantum ground states, $|\downarrow\rangle$ ($|\uparrow\rangle$), have N_0 ($N_0 - 2$) particles in the condensate and empty (filled) pairs of Majorana modes, thus encoding a qubit [13, 44]. It is this topological degeneracy which will lead to the effective spin degeneracy for the effective Kondo model. Now, we assume, no overlap between the MBS, hence the degeneracy remains exact, otherwise a “Zeeman coupling” [15] term can arise.

The TKE occurs when the MCB is coupled to conduction electrons through external metallic leads as shown in Fig. 2. We work at the energy scales much smaller than the superconducting gap, as well as below the energies of any other subgap excitations of non-Majorana character. At such temperatures the subgap states are not populated and can be ignored. Then, the Hamiltonian of the system is given by $H_{TK} = H_{cond} + H_c + H_{tun}$, where H_{cond} is the Hamiltonian of the conduction electrons of the leads. The tunneling Hamiltonian H_{tun} describes the low-energy coupling between the leads and the MCB island. H_{tun} is given by

$$H_{tun} = \exp(i\phi/2) \sum_{j=1}^3 t_{jj} \gamma_j \psi_j + \text{H.c.}, \quad (6)$$

where ϕ is the phase of the superconducting order parameter, t_{jj} is the tunneling amplitude, ψ_j is the electron annihilation operator and γ_j is the Majorana operator at lead j . Such tunneling process explicitly excludes the possibility of exciting quasiparticles [45]. As was demonstrated in [13, 46], if the charging energy of the box is much greater than the characteristic value of the tunneling matrix elements, i.e. if $E_C \gg t_j$, one can integrate out the phase fluctuations of the condensate which results in the exchange interaction between such MCB and the electrons of the leads (it is supposed that they are spin polarized):

$$H_{ex} = J_K^{ij} (\psi_i^\dagger \psi_j - \psi_j^\dagger \psi_i) \gamma_i \gamma_j, \quad J_K^{ij} \sim t_i t_j / E_C, \quad (7)$$

where indices i, j correspond to the leads. For a single MCB this interaction gives rise to the TKE, where the leads serve as the bulk. The spin operator S^i realized by the Majorana operators is

$$S^i = \frac{i}{2} \epsilon_{ijk} \gamma_j \gamma_k, \quad \{\gamma_k, \gamma_j\} = \delta_{jk}. \quad (8)$$

The model comprised of the lead Hamiltonian and the effective exchange Hamiltonian [Eqn.(7)] defines an antiferromagnetic Kondo problem.

In the limit of isotropic couplings, where all of the J_K^{ij} s are same, implying $J_K^{12} = J_K^{23} = J_K^{13}$, one arrives at the RG flow equations of the isotropic Kondo problem. In this limit, the

Topological Kondo temperature T_K at which the perturbation theory breaks down due to the RG flow towards strong coupling is given by [13–15],

$$T_K \sim E_c \exp(-1/\rho \bar{J}_K), \quad (9)$$

where ρ is the density of states of the lead electrons at the Fermi energy and $J_K^{12} = J_K^{23} = J_K^{13} = \bar{J}_K$ is the average bare value of the exchange coupling. Consequently, T_K sets an energy scale between the trivial regime and the Topological Kondo regime, below which a robust non-Fermi liquid (NFL) behavior can be observed. However, a strong exponential factor in Eqn.(9) can drive the temperature for the TKE to zero. In deriving T_K [Eqn.(9)], a possibility of hybridization between the MBS has been ignored. If the hybridization of the form $H_{hyb} = i \sum_{j \neq k} h_{jk} \gamma_j \gamma_k$ is present, the TKE will be then observed in a temperature window $T_{hyb} < T < T_K$, where $T_{hyb} = T_K (\bar{h}/T_K)^{M/2}$ [15], with $\bar{h} = \max|h_{jk}|$.

Anisotropies [15] in the exchange couplings are marginal perturbations so the NFL fixed point of TKE remains robust [14, 47]. In the following, we consider the anisotropic case when $J_K^{12} = J_K^{13} \neq J_K^{23}$. In the new notations $J_K^{12} = J_K^{13} \equiv J_\perp$ and $J_K^{23} \equiv J_\parallel$. The one-loop perturbative RG equations in this case are,

$$\frac{dJ_\parallel}{d \log \Lambda} = -\rho J_\perp^2 \quad (10)$$

$$\frac{dJ_\perp}{d \log \Lambda} = -\rho J_\parallel J_\perp. \quad (11)$$

From the above RG equations Eqn.(10) one finds that,

$$\begin{aligned} \frac{dJ_\parallel}{dJ_\perp} &= \frac{J_\perp}{J_\parallel} \\ \Rightarrow J_\parallel^2 - J_\perp^2 &= C \end{aligned} \quad (12)$$

Eqn.(12) represents a scaling constraint to be obeyed, where C is a real constant. Next, plugging in Eqn.(12) in Eqn.(10), we obtain

$$\frac{dJ_\parallel}{d \log \Lambda} = -\rho (J_\parallel^2 - C). \quad (13)$$

To obtain the Topological Kondo energy scale, we integrate the above RG equation [Eqn.(13)]. Following the approach in [13], the energy cutoff or the effective bandwidth Λ varies between $[T_K, D]$, where $D \sim E_c$, where E_c is the charging energy of the island. There are two regimes $C > 0$ and $C < 0$. T_K will give the Topological Kondo temperature, at which the coupling constants flow to strong-coupling which for the estimate purposes we can treat as infinity.

We assume that $\rho \sqrt{|C|} \ll 1$. Then for $C > 0$ we obtain

$$T_K \sim E_c \left(\frac{-\sqrt{C} + J_\parallel(0)}{\sqrt{C} + J_\parallel(0)} \right)^{1/2\rho\sqrt{C}}, \quad (14)$$

Here, we see that to have a greater T_K it is advantageous for

us to have strong anisotropy $J_{\parallel} \gg J_{\perp}$ which corresponds to the situation when one of the tunneling integrals t_i is much smaller than two others.

For $C < 0$ we have

$$T_K \sim E_c \exp \left[\frac{-1}{\rho \sqrt{|C|}} (\pi/2 - \tan^{-1}(J_{\parallel}(0)/\sqrt{|C|})) \right] \quad (15)$$

, where $J_{\parallel}(0)$ is the bare coupling.

One problem is that in all cases apart from tunneling into MBS (6) there may be a direct tunneling of bulk electrons into the superconductor. There are, however, reasons why this process is irrelevant. Indeed, the corresponding Hamiltonian is

$$H_{tun,2} = g \left[A_{lj} \exp(i\phi) \psi_l \psi_j + H.c. \right], \quad A_{lj} = -A_{jl}. \quad (16)$$

When we integrate over ϕ , however, the result is a local four fermion interaction

$$V \sim \frac{g^2}{E_c} A_{lj} A_{l'j'} \psi_l \psi_j \psi_{l'}^* \psi_{j'}^*, \quad (17)$$

which is highly irrelevant.

Below we give estimates of the parameters pertinent to the realization of TKE for the device setup depicted in Fig.2.

We start by summarizing the criteria to be satisfied are: (i) four well-localized MBS, (ii) the MBS must be well-separated, such that the hybridization between them is insignificant, but fit inside the Coulomb box, (iii) a charging energy E_c of the order of the superconducting gap Δ . These conditions can be expressed in the sequence of inequalities:

$$\Delta_0 \gg E_c \gg t_i, \quad C \sim L \gg \lambda. \quad (18)$$

The decay length of the MBS is given by $\lambda = \frac{v_m}{\Delta_0}$ [38], where v_m is given by Eq.(4). To make it to be much smaller than the size (L) of the Coulomb box we need to reduce v_m . For $\text{FeSe}_{0.45}\text{Te}_{0.55}$, with typical values of $v_F \sim 216 \text{ meV \AA}$ [21], $\Delta_0 \sim 1.8 \text{ meV}$, $\mu \sim 5\Delta_0$ ($\mu \gg \Delta_0$), the smallest value of $v_m \approx v_F(\Delta_0/\mu)^3$, λ of order of 1 \AA is achieved when $k_F W = \pi(1+2n)/2$. It is important to note that the decay length λ is well below the superconducting coherence length of the Fe(Se,Te) [48, 49], which is required for the stability of the MBS.

With a superconducting island of area $A \sim 60 \text{ nm} \times 60 \text{ nm}$ and thickness $d \sim 1 \text{ nm}$, and assuming permittivity of an insulating material being $\epsilon \sim 2 \times 55e^2 ev^{-1}(\mu\text{m})^{-1}$, the charging energy $E_c = \frac{e^2}{2C}$, with $C = \frac{\epsilon A}{d}$ will be of the order of $1.38 \text{ meV} \equiv 16K \sim \Delta_0$. Hence we notice that, the device geometry can achieve a large upper-bound for the topological Kondo temperature scale, while remaining in the superconducting state. We also see that the effective Topological Kondo temperature is determined not just by E_c , but also by the tunneling integrals t_i which enter into the expressions for the exchange integrals. Thus, even a suppression due to the exponential factor, can result in a relatively larger T_K , as long as E_c is large. The suppression will depend on the density of

states of the metallic lead-electrons and the nature of the contacts used. Therefore, we see that a mesoscopic MCB island with well-separated and localized MBS can be achieved with a large T_K [see for e.g. Eqn.(9)]. As the T_K achieved in the Fe(Se,Te) based device can be significantly higher than the heterostructures systems based on semiconductor nanowire and conventional superconductors [13], this device will significantly improve the experimental feasibility of the TKE.

As we have mentioned in the introduction, that one possible way to detect the TKE is to measure the conductance between different leads, as the TKE leads to unusual temperature dependencies for the two-terminal linear conductance σ_{ij} ($i \neq j$) [14, 15]. In the temperature-regime larger than T_K , the σ_{ij} grows as $\frac{1}{\ln^2(T/T_K)}$ with lowering the temperature. For temperature-regime smaller than T_K , σ_{ij} approaches the universal value $\frac{2e^2}{3h}$ with $(T/T_K)^{2/3}$ temperature dependence. Both the universal value and the temperature dependence of the conductance are unique characteristics of the NFL ground state providing an alternative pathway for detecting the Majorana fermions in the Fe(Se,Te) based device. Moreover, the signature of the TKE can also be found in the tunneling measurements for example using STM. Ref. [50] describes the situation when the leads are one-dimensional wires with the Luttinger parameter K . In the presence of the TKE, the local density of states (LDOS) $\rho(\omega)$ of the lead-electrons close to the MCB island, as a function of the energy has a dependence $\rho(\omega) \sim \omega^{\frac{1}{MK}[1+(M-1)K^2]-1}$ [50], where K is related to the Coulomb repulsion between electrons in the lead. Hence, depending on the strength of the interaction among the electrons in the metallic lead, the LDOS will show unique features, which can provide an alternative experimental route to find signature of the TKE.

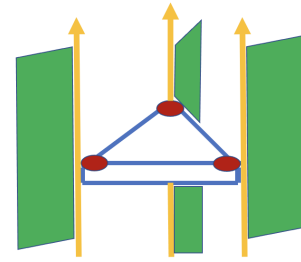


FIG. 3: A schematic depiction of the arrangement for the Chiral Kondo effect. The triangle is the superconducting (Cooper pair) box, the red dots are Majorana zero modes coupled by tunneling to chiral edges of topological insulators.

Arrays of TKE: We conclude our paper with a brief description of a device which can incorporate multiple anyons. This is chiral Kondo lattice first described in [10, 51, 52]. Here the itinerant electrons are chiral, they move in one direction and hence such lattice does not have Ruder- man–Kittel–Kasuya–Yosida (RKKY) interaction. In fact, it is equivalent to the bunch of impurities and as a consequence the ground state remains critical as for the single impurity case.

Chiral Kondo lattice for Topological Kondo effect can serve as a platform for anyon-based quantum computation [10, 51, 52]. An elementary block of such Kondo lattice is de-

picted on Fig.(3). The suitable material for chiral edges containing polarized electrons is MnBi_2Te_4 [53], which is distinguished by a relatively large bulk gap, allowing one to operate at temperatures of order of several degrees.

IV. SUMMARY

In this work, we have provided a new potential route to achieve the Topological Kondo effect (TKE) through various iron-based superconductors such as $\text{FeSe}_{0.45}\text{Te}_{0.55}$ [$\text{Fe}(\text{Se},\text{Te})$] based Majorana-Cooper boxes (MCB). The proposed device set up has two marked differences from the ear-

lier proposals set ups which include heterostructures containing semiconductor nanowires proximitized to conventional superconductors. First, there is a significant enhancement of the Topological Kondo temperature scale and the second, there is a simplification of the device structure.

V. ACKNOWLEDGEMENTS

This work was supported by U.S. Department of Energy (DOE) the Office of Basic Energy Sciences, Materials Sciences and Engineering Division under Contract No. DE-SC0012704.

[1] C. Nayak, S. H. Simon, A. Stern, M. Freedman, and S. Das Sarma, Non-abelian anyons and topological quantum computation, *Rev. Mod. Phys.* **80**, 1083 (2008).

[2] P. Nozieres and A. Blandin, Kondo effect in real metals, *Journal de Physique* **41**, 193 (1980).

[3] A. Tsvelick and P. Wiegmann, Solution of the n-channel kondo problem (scaling and integrability), *Zeitschrift für Physik B Condensed Matter* **54**, 201 (1984).

[4] I. Affleck and A. W. Ludwig, The kondo effect, conformal field theory and fusion rules, *Nuclear Physics B* **352**, 849 (1991).

[5] R. Potok, I. Rau, H. Shtrikman, Y. Oreg, and D. Goldhaber-Gordon, Observation of the two-channel kondo effect, *Nature* **446**, 167 (2007).

[6] A. Keller, L. Peeters, C. Moca, I. Weymann, D. Mahalu, V. Umansky, G. Zaránd, and D. Goldhaber-Gordon, Universal fermi liquid crossover and quantum criticality in a mesoscopic system, *Nature* **526**, 237 (2015).

[7] Z. Iftikhar, S. Jezouin, A. Anthore, U. Gennser, F. Parmentier, A. Cavanna, and F. Pierre, Two-channel kondo effect and renormalization flow with macroscopic quantum charge states, *Nature* **526**, 233 (2015).

[8] Z. Iftikhar, A. Anthore, A. Mitchell, F. Parmentier, U. Gennser, A. Ouerghi, A. Cavanna, C. Mora, P. Simon, and F. Pierre, Tunable quantum criticality and super-ballistic transport in a “charge” kondo circuit, *Science* **360**, 1315 (2018).

[9] D. Karki, E. Boulat, W. Pouse, D. Goldhaber-Gordon, A. K. Mitchell, and C. Mora, Z 3 parafermion in the double charge kondo model, *Physical Review Letters* **130**, 146201 (2023).

[10] P. L. S. Lopes, I. Affleck, and E. Sela, Anyons in multichannel kondo systems, *Phys. Rev. B* **101**, 085141 (2020).

[11] Y. Komijani, Isolating kondo anyons for topological quantum computation, *Phys. Rev. B* **101**, 235131 (2020).

[12] Y. Ge and Y. Komijani, Emergent spinon dispersion and symmetry breaking in two-channel kondo lattices, *Phys. Rev. Lett.* **129**, 077202 (2022).

[13] B. Béri and N. R. Cooper, Topological kondo effect with majorana fermions, *Phys. Rev. Lett.* **109**, 156803 (2012).

[14] A. Altland and R. Egger, Multiterminal coulomb-majorana junction, *Phys. Rev. Lett.* **110**, 196401 (2013).

[15] A. Altland, B. Béri, R. Egger, and A. M. Tsvelik, Multichannel kondo impurity dynamics in a majorana device, *Phys. Rev. Lett.* **113**, 076401 (2014).

[16] J. I. Väyrynen, A. E. Feiguin, and R. M. Lutchyn, Signatures of topological ground state degeneracy in majorana islands, *Phys. Rev. Res.* **2**, 043228 (2020).

[17] D. Liu, Z. Cao, X. Liu, H. Zhang, and D. E. Liu, Topological kondo device for distinguishing quasi-majorana and majorana signatures, *Phys. Rev. B* **104**, 205125 (2021).

[18] C. Beenakker, Search for majorana fermions in superconductors, *Annu. Rev. Condens. Matter Phys.* **4**, 113 (2013).

[19] M. Sato and Y. Ando, Topological superconductors: a review, *Reports on Progress in Physics* **80**, 076501 (2017).

[20] G. Xu, B. Lian, P. Tang, X.-L. Qi, and S.-C. Zhang, Topological superconductivity on the surface of fe-based superconductors, *Phys. Rev. Lett.* **117**, 047001 (2016).

[21] D. Wang, L. Kong, P. Fan, H. Chen, S. Zhu, W. Liu, L. Cao, Y. Sun, S. Du, J. Schneeloch, R. Zhong, G. Gu, L. Fu, H. Ding, and H.-J. Gao, Evidence for majorana bound states in an iron-based superconductor, *Science* **362**, 333 (2018).

[22] P. Zhang, K. Yaji, T. Hashimoto, Y. Ota, T. Kondo, K. Okazaki, Z. Wang, J. Wen, G. Gu, H. Ding, *et al.*, Observation of topological superconductivity on the surface of an iron-based superconductor, *Science* **360**, 182 (2018).

[23] T. Machida, Y. Sun, S. Pyon, S. Takeda, Y. Kohsaka, T. Hanaguri, T. Sasagawa, and T. Tamegai, Zero-energy vortex bound state in the superconducting topological surface state of fe (se, te), *Nature materials* **18**, 811 (2019).

[24] Q. Liu, C. Chen, T. Zhang, R. Peng, Y.-J. Yan, C.-H.-P. Wen, X. Lou, Y.-L. Huang, J.-P. Tian, X.-L. Dong, G.-W. Wang, W.-C. Bao, Q.-H. Wang, Z.-P. Yin, Z.-X. Zhao, and D.-L. Feng, Robust and clean majorana zero mode in the vortex core of high-temperature superconductor $(\text{Li}_{0.84}\text{Fe}_{0.16})\text{OHFeSe}$, *Phys. Rev. X* **8**, 041056 (2018).

[25] W. Liu, L. Cao, S. Zhu, L. Kong, G. Wang, M. Papaj, P. Zhang, Y.-B. Liu, H. Chen, G. Li, *et al.*, A new majorana platform in an fe-as bilayer superconductor, *Nature Communications* **11**, 5688 (2020).

[26] J.-X. Yin, Z. Wu, J. Wang, Z. Ye, J. Gong, X. Hou, L. Shan, A. Li, X. Liang, X. Wu, *et al.*, Observation of a robust zero-energy bound state in iron-based superconductor fe (te, se), *Nature Physics* **11**, 543 (2015).

[27] S. Zhu, L. Kong, L. Cao, H. Chen, M. Papaj, S. Du, Y. Xing, W. Liu, D. Wang, C. Shen, *et al.*, Nearly quantized conductance plateau of vortex zero mode in an iron-based superconductor, *Science* **367**, 189 (2020).

[28] J. Alicea, New directions in the pursuit of majorana fermions in solid state systems, *Reports on progress in physics* **75**, 076501 (2012).

[29] C. Caroli, P. De Gennes, and J. Matricon, Bound fermion states on a vortex line in a type ii superconductor, *Physics Letters* **9**,

307 (1964).

[30] L. Kong, S. Zhu, M. Papaj, H. Chen, L. Cao, H. Isobe, Y. Xing, W. Liu, D. Wang, P. Fan, *et al.*, Half-integer level shift of vortex bound states in an iron-based superconductor, *Nature Physics* **15**, 1181 (2019).

[31] K. Jiang, X. Dai, and Z. Wang, Quantum anomalous vortex and majorana zero mode in iron-based superconductor fe(te,se), *Phys. Rev. X* **9**, 011033 (2019).

[32] S. S. Zhang, J.-X. Yin, G. Dai, L. Zhao, T.-R. Chang, N. Shumiya, K. Jiang, H. Zheng, G. Bian, D. Multer, M. Litskevich, G. Chang, I. Belopolski, T. A. Cochran, X. Wu, D. Wu, J. Luo, G. Chen, H. Lin, F.-C. Chou, X. Wang, C. Jin, R. Sankar, Z. Wang, and M. Z. Hasan, Field-free platform for majorana-like zero mode in superconductors with a topological surface state, *Phys. Rev. B* **101**, 100507 (2020).

[33] C. Liu, C. Chen, X. Liu, Z. Wang, Y. Liu, S. Ye, Z. Wang, J. Hu, and J. Wang, Zero-energy bound states in the high-temperature superconductors at the two-dimensional limit, *Science advances* **6**, eaax7547 (2020).

[34] P. Fan, F. Yang, G. Qian, H. Chen, Y.-Y. Zhang, G. Li, Z. Huang, Y. Xing, L. Kong, W. Liu, *et al.*, Observation of magnetic adatom-induced majorana vortex and its hybridization with field-induced majorana vortex in an iron-based superconductor, *Nature communications* **12**, 1348 (2021).

[35] C. Chen, K. Jiang, Y. Zhang, C. Liu, Y. Liu, Z. Wang, and J. Wang, Atomic line defects and zero-energy end states in monolayer fe (te, se) high-temperature superconductors, *Nature Physics* **16**, 536 (2020).

[36] Z. Wang, J. O. Rodriguez, L. Jiao, S. Howard, M. Graham, G. Gu, T. L. Hughes, D. K. Morr, and V. Madhavan, Evidence for dispersing 1d majorana channels in an iron-based superconductor, *Science* **367**, 104 (2020).

[37] N. Zaki, G. Gu, A. Tsvelik, C. Wu, and P. D. Johnson, Time-reversal symmetry breaking in the fe-chalcogenide superconductors, *Proceedings of the National Academy of Sciences* **118**, e2007241118 (2021).

[38] R. Song, P. Zhang, and N. Hao, Phase-manipulation-induced majorana mode and braiding realization in iron-based superconductor fe(te,se), *Phys. Rev. Lett.* **128**, 016402 (2022).

[39] M. H. Christensen, J. Kang, and R. M. Fernandes, Intertwined spin-orbital coupled orders in the iron-based superconductors, *Phys. Rev. B* **100**, 014512 (2019).

[40] E. Mascot, S. Cocklin, M. Graham, M. Mashkoori, S. Rachel, and D. K. Morr, Topological surface superconductivity in fese0.45te0.55, *Communications Physics* **5**, 188 (2022).

[41] S. Sarkar, J. Van Dyke, P. O. Sprau, F. Massee, U. Welp, W.-K. Kwok, J. C. S. Davis, and D. K. Morr, Orbital superconductivity, defects, and pinned nematic fluctuations in the doped iron chalcogenide fese_{0.45}te_{0.55}, *Phys. Rev. B* **96**, 060504 (2017).

[42] L. Fu and C. L. Kane, Superconducting proximity effect and majorana fermions at the surface of a topological insulator, *Phys. Rev. Lett.* **100**, 096407 (2008).

[43] C.-X. Liu, D. E. Liu, F.-C. Zhang, and C.-K. Chiu, Protocol for reading out majorana vortex qubits and testing non-abelian statistics, *Phys. Rev. Appl.* **12**, 054035 (2019).

[44] L. Fu, Electron teleportation via majorana bound states in a mesoscopic superconductor, *Phys. Rev. Lett.* **104**, 056402 (2010).

[45] S. Plugge, A. Zazunov, E. Eriksson, A. M. Tsvelik, and R. Egger, Kondo physics from quasiparticle poisoning in majorana devices, *Phys. Rev. B* **93**, 104524 (2016).

[46] M. R. Galpin, A. K. Mitchell, J. Temaismithi, D. E. Logan, B. Béri, and N. R. Cooper, Conductance fingerprint of majorana fermions in the topological kondo effect, *Phys. Rev. B* **89**, 045143 (2014).

[47] A. Zazunov, A. Altland, and R. Egger, Transport properties of the coulomb-majorana junction, *New Journal of Physics* **16**, 015010 (2014).

[48] A. Audouard, F. Duc, L. Drigo, P. Toulemonde, S. Karlsson, P. Strobel, and A. Sulpice, Quantum oscillations and upper critical magnetic field of the iron-based superconductor fese, *Europhysics Letters* **109**, 27003 (2015).

[49] U. R. Singh, S. C. White, S. Schmaus, V. Tsurkan, A. Loidl, J. Deisenhofer, and P. Wahl, Evidence for orbital order and its relation to superconductivity in fese0.4te0.6, *Science Advances* **1**, e1500206 (2015).

[50] E. Eriksson, A. Nava, C. Mora, and R. Egger, Tunneling spectroscopy of majorana-kondo devices, *Phys. Rev. B* **90**, 245417 (2014).

[51] D. Gabay, C. Han, P. L. S. Lopes, I. Affleck, and E. Sela, Multi-impurity chiral kondo model: Correlation functions and anyon fusion rules, *Phys. Rev. B* **105**, 035151 (2022).

[52] M. Lotem, E. Sela, and M. Goldstein, Manipulating non-abelian anyons in a chiral multichannel kondo model, *Phys. Rev. Lett.* **129**, 227703 (2022).

[53] Z. Ying, S. Zhang, B. Chen, B. Jia, F. Fei, M. Zhang, H. Zhang, X. Wang, and F. Song, Experimental evidence for dissipationless transport of the chiral edge state of the high-field chern insulator in mnbi₂te₄ nanodevices, *Phys. Rev. B* **105**, 085412 (2022).